

# Simulation of a fixed cylinder in waves using the SWENSE method within a weakly-compressible approach

M. Gouin\* <sup>1,2</sup>, G. Oger <sup>1</sup> and D. Le Touzé <sup>1</sup>

1. Ecole Centrale Nantes, LHEEA Research Dept., UMR CNRS 6598, Nantes, France

2. Institut de Recherche Technologique Jules Verne, Bouguenais, France

E-mail : maite.gouin@ec-nantes.fr

## Highlights

- Development of the SWENSE method within a monophasic weakly-compressible Navier-Stokes solver.
- Application of the SWENSE method to a fixed cylinder in a regular wave field.

## Introduction

Naval or ocean engineering hydrodynamic problems are usually solved using either potential flow assumption or the full Navier-Stokes equations. Potential flow solvers provide very fast and accurate results for propagating gravity waves, but cannot describe the interaction of these waves with structures when viscosity/turbulence play a significant role. On the contrary, Computational Fluid Dynamics (CFD) solvers can accurately predict fluid/structure interactions but are not fully adapted to wave propagation cases because of their inherent numerical diffusion.

The purpose of this work is to combine the advantages of potential flow and CFD solutions through the use of a hybrid SWENSE (Spectral Wave Explicit Navier-Stokes Equations) method. The essence of this method is to pre-calculate the incident flow (waves and/or currents) through a potential flow spectral solver and to insert it within the Navier-Stokes equations to get the SWENSE equations. As a result, only the disturbed flow solution is computed. This kind of hybridization was first introduced in [4] and then extended in [5, 12, 14, 16].

The disturbed flow (diffracted + radiated + viscous + turbulent) is mainly located in the structure vicinity. Thus, only the near-structure area needs a fine spatial resolution, saving large computational time and making the SWENSE formalism very attractive. An alternative to the SWENSE method is to directly force wave boundary conditions at the boundary of a reduced Navier-Stokes domain as presented for instance in [15]. Such a one-way coupled method is interesting because of its relative simplicity. Nevertheless, it presents some drawbacks: the wave propagation is more difficult to simulate accurately in the Navier-Stokes domain and the method needs much larger refined computational domains.

In the present work we propose to extend the SWENSE method to an in-house Finite Volume Navier-Stokes solver based on a weakly-compressible approach [2]. It is still under development and is already able to model viscous and turbulent flows including complex moving geometries. A fully explicit temporal scheme combined with the weakly-compressible approach is used and a purely Cartesian grid is adopted for numerical accuracy and algorithmic simplicity purposes. An Adaptive Mesh Refinement (AMR) method embedded within a massively parallel framework is implemented and geometries are automatically immersed within the Cartesian grid, preventing the need for complex pre-processing tools as needed in body-fitted strategies for instance.

In the present context, the SWENSE method needs to be adapted to a weakly-compressible formulation of the Navier-Stokes equations whereas it was only derived under the incompressible assumption in previous works [4, 5, 12, 14, 16]. As for the incompressible version, only the disturbed solution needs to be finally computed, in addition to advection terms of the disturbed solution along the imposed incident velocity, as presented in the first part of this paper. To our knowledge, such an implementation of the SWENSE method within a weakly-compressible solver has never been proposed so that it represents both a numerical challenge and an original topic. The final objective will be to impose the incident flow as a highly accurate wave solution (Rienecker & Fenton [17], High Order Spectral (HOS) [3] possibly taking into account variable bathymetry as proposed in [6]), so as to solve practical engineering problems. Nevertheless, for validations purposes, some very simple incident flows are used in this paper in a first attempt: the propagation of an Airy wave past a cylinder is presented and comparisons are performed with experimental and numerical results.

## Numerical model

### Weakly-compressible Navier-Stokes solver

The CFD solver used in this work aims at solving the following Navier-Stokes equations:

$$\frac{\partial \rho}{\partial t} + \nabla \cdot (\rho \mathbf{u}) = 0, \quad (1)$$

$$\frac{\partial (\rho \mathbf{u})}{\partial t} + \nabla \cdot (\rho \mathbf{u} \otimes \mathbf{u}) = -\nabla p + \rho \mathbf{g} + \mu \nabla^2 \mathbf{u}, \quad (2)$$

where  $\mathbf{g}$ ,  $\rho$ ,  $\mu$ ,  $p$ ,  $\mathbf{u}$  are respectively the gravity, density, dynamic viscosity, pressure and velocity.  $p$  is deduced from the following Equation Of State (EOS) which depends exclusively on the density as:

$$p - p_0 = \frac{\rho_0 c_0^2}{\gamma} \left[ \left( \frac{\rho}{\rho_0} \right)^\gamma - 1 \right] = EOS(\rho), \quad (3)$$

where  $p_0$  is a reference pressure taken here as  $p_0 = 0$ .  $\rho_0$  is the nominal density,  $c_0$  is the nominal sound speed and  $\gamma$  is the polytropic constant. The sound speed  $c_0$  should be chosen to fulfill the weakly-compressible assumption, as discussed in [2] [13]. In the following, the system (1)-(2) is decomposed into an hyperbolic part (Euler equations) and a viscous part. The hyperbolic flux computation can be performed by using any exact or approached Riemann solver. The flux is computed from the left and right states at each cell edge, these states being reconstructed from the surrounding cells values using either a MUSCL scheme [10] or a WENO scheme [11, 19]. The viscous fluxes are computed by applying the method proposed in [1] (see [2] for more details). The SWENSE method introduced hereafter exclusively uses a 5<sup>th</sup> order WENO scheme for accuracy purposes.

## SWENSE formalism proposed

Starting from the above formalism, the SWENSE method is derived as follows: first, the Navier-Stokes equations are re-written with "total" variables. Then, the incident (undisturbed) flow part is subtracted from the total flow and some terms naturally vanish since the incident field fulfills the mass and momentum conservation equations under the incompressible hypothesis. Re-writing the Navier-Stokes equations with total variables leads to:

$$\frac{\partial \rho_T}{\partial t} + \nabla \cdot (\rho_T \mathbf{u}_T) = 0, \quad (4)$$

$$\frac{\partial (\rho_T \mathbf{u}_T)}{\partial t} + \nabla \cdot (\rho_T \mathbf{u}_T \otimes \mathbf{u}_T) = -\nabla p_T + \rho_T \mathbf{g} + \mu \nabla^2 \mathbf{u}_T, \quad (5)$$

$$p_T = EOS(\rho_T), \quad (6)$$

where the total velocity field respects  $\mathbf{u}_T = \mathbf{u}_I + \mathbf{u}_D$ , in which subscripts  $T$ ,  $I$  and  $D$  refer to the total, incident and disturbed fields respectively. The incident flow is always taken as incompressible, inviscid and irrotational in the present work, so that:

$$\rho_I = \rho_0 = cst, \quad (7)$$

$$\nabla \cdot (\rho_0 \mathbf{u}_I) = 0, \quad (8)$$

$$\frac{\partial (\rho_0 \mathbf{u}_I)}{\partial t} + \nabla \cdot (\rho_0 \mathbf{u}_I \otimes \mathbf{u}_I) = -\nabla p_I + \rho_0 \mathbf{g}. \quad (9)$$

From Eq.(4-6) and Eq.(7-9), and noting  $\mathbf{u}_D = \mathbf{u}_T - \mathbf{u}_I$  and  $p_D = p_T - p_I$ , we deduce:

$$\frac{\partial \rho_T}{\partial t} + \nabla \cdot (\rho_T \mathbf{u}_D) + \mathbf{u}_I \cdot \nabla \rho_T = 0, \quad (10)$$

$$\begin{aligned} & \frac{\partial (\rho_T \mathbf{u}_D)}{\partial t} + \nabla \cdot [\rho_T \mathbf{u}_D \otimes \mathbf{u}_D] + \nabla \cdot [\rho_T \mathbf{u}_D \otimes \mathbf{u}_I] + \nabla \cdot [\rho_T \mathbf{u}_I \otimes \mathbf{u}_D] \\ &= -\frac{\partial (\mathbf{u}_I (\rho_T - \rho_0))}{\partial t} - \nabla \cdot [(\rho_T - \rho_0) \mathbf{u}_I \otimes \mathbf{u}_I] + (\rho_T - \rho_0) \mathbf{g} - \nabla p_D + \mu \nabla^2 \mathbf{u}_D, \end{aligned} \quad (11)$$

$$p_D = EOS(\rho_T), \quad (12)$$

where  $\nabla^2 \mathbf{u}_I = 0$  ( $\nabla \times \mathbf{u}_I = 0$  since we assumed an incident irrotational potential flow), and  $EOS(\rho_I) = EOS(\rho_0) = 0$ . Noting  $\Delta \rho = \rho_T - \rho_0$ , the term written in blue can be decomposed as:

$$-\underbrace{\mathbf{u}_I \frac{\partial \Delta \rho}{\partial t}}_{(1)} - \underbrace{\Delta \rho \frac{\partial \mathbf{u}_I}{\partial t}}_{(2)} - \underbrace{\Delta \rho \nabla \cdot [\mathbf{u}_I \otimes \mathbf{u}_I]}_{(3)} - \underbrace{(\mathbf{u}_I \otimes \mathbf{u}_I) \nabla \cdot [\Delta \rho]}_{(4)} + \underbrace{\Delta \rho \mathbf{g}}_{(5)} \quad (13)$$

In the weakly-compressible case ( $Ma < 0.1$ , see [2] for more details) the density remains very close to the nominal density ( $\Delta \rho < 0.01$ ), so that:  $\rho_T \simeq \rho_0 \simeq \rho_D$ . We thus make the hypothesis that:

$$\rho = \rho_D = \rho_T = \rho_0, \quad (14)$$

so that all the terms in Eq.(13) vanish. The final set of equations can be approximated as:

$$\frac{\partial \rho}{\partial t} + \nabla \cdot (\rho \mathbf{u}_D) + \mathbf{u}_I \cdot \nabla \rho = 0, \quad (15)$$

$$\frac{\partial (\rho \mathbf{u}_D)}{\partial t} + \nabla \cdot [\rho \mathbf{u}_D \otimes \mathbf{u}_D] + \nabla \cdot [\rho \mathbf{u}_D \otimes \mathbf{u}_I] + \nabla \cdot [\rho \mathbf{u}_I \otimes \mathbf{u}_D] = -\nabla p_D + \mu \nabla^2 \mathbf{u}_D, \quad (16)$$

$$p_D = EOS(\rho), \quad (17)$$

The terms in red represent the additional terms compared to Eq.(1) and Eq.(2). More details about the discrete formulation are given in [7].

# Application: Fixed cylinder in an Airy wave

## Test case presentation

The case of a cylinder immersed in an Airy wave is studied in this section. There is no influence of the free-surface since the cylinder is located far from it, in addition to its location nearby the floor. We use here the experimental configuration from Jarno-Druaux et al. [9]. The steepness is  $ka = 0.1$  and the relative water depth is  $kh = 1.14$ . Following the Le Méhauté diagram, a third order theory (at least) is required in this case but the wave field is generated here using an Airy wave as the cylinder is located far from the free-surface (and as presented in the numerical simulations of [8]). The computed maximum horizontal velocity  $U_m$  at  $t/T = 0$  within the region extending from 0.01 to 0.03m from the bottom is about 0.09m/s (following [21]). The Reynolds number is  $Re = \frac{U_m D}{\nu} = 1800$  and the Keulegan-Carpenter number  $KC = \frac{U_m T}{D}$  is about 4.9.  $e/D = 0.5$  so that the cylinder is out of the boundary layer (the thickness of the boundary layer is  $\delta \simeq 0.003m$ ).

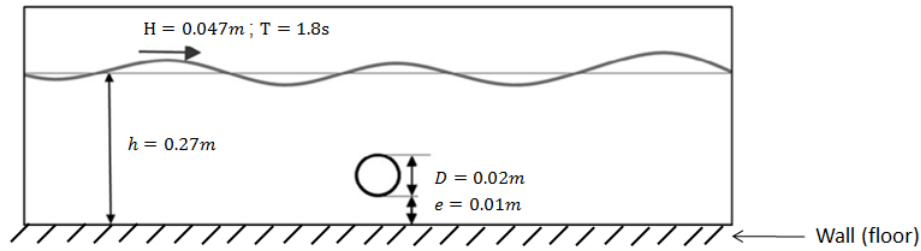


Figure 1: Fixed cylinder in Airy wave: sketch of the experimental configuration from [9].

The WCCH-SWENSE domain is discretized between  $-0.07m$  and  $-0.27m$  in the  $y$ -direction. and the mesh is refined locally around the cylinder. The converged results with the IH2VOF model [8] were obtained with 50 cells per diameter in each direction, i.e. a minimum mesh size of 0.4mm. In [21] the results are presented with a minimum mesh size of 0.1mm in the vertical direction. In our case, the convergence for  $Ma \leq 0.05$  is obtained with 200 cells per diameter (corresponding to 526400 cells in the whole domain).

## Comparison between experimental and numerical results

Experimental velocities were measured using a Doppler velocimeter and were averaged over 15 wave periods. For comparison purposes, the present simulation was also run and averaged during 15 wave periods. The instant  $t/T = 0$  corresponds to the instant when a crest is located right above the cylinder (see [8]) which corresponds in our case to  $t = 0.51s$ . In Fig.2 the present results are compared to the experimental snapshots presented in [9]. We clearly observe the generation of vortices predicted by the theory (see [18]) and our results are similar to the experimental ones. As expected, the numerical solution provides some more details of this complex flow. Indeed, small structures which were not captured by the experimental device can be observed numerically in the near cylinder area.

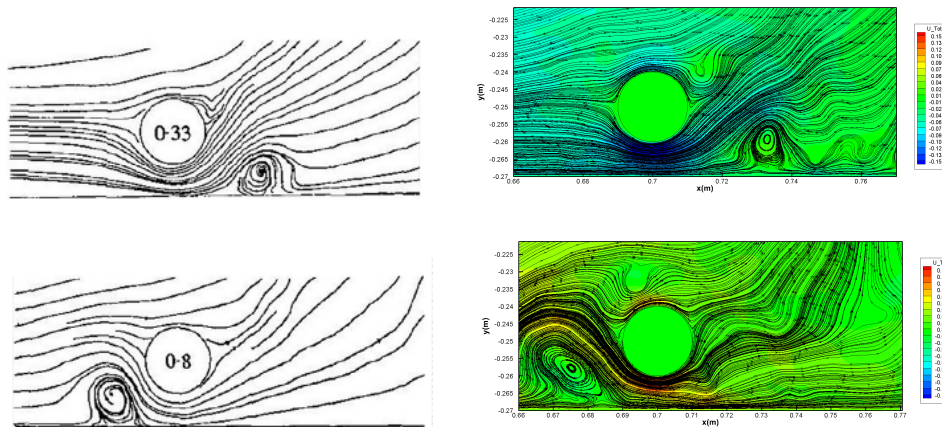


Figure 2: Fixed cylinder in Airy wave: Snapshots at  $t/T = 0.33$  and  $t/T = 0.8$ . Left: experimental streamlines from [9] averaged over 15 periods - Right: numerical streamlines obtained with WCCH-SWENSE for 200 cells per diameter averaged over 15 periods.

Fig.3 presents a comparison of the WCCH-SWENSE results with the numerical solutions from [8] and [21] (instantaneous streamlines). A good agreement is observed with the results from [21]. Moreover, it seems that WCCH-SWENSE is able to capture more complex phenomena and details than the model used in [21], even with the same spatial resolution within the cylinder, showing the ability of the present WCCH-SWENSE model to capture more accurately some small structures present within these vortex sheddings. The model from [8] shows some differences with both the WCCH-SWENSE method and the FEM model in [21].

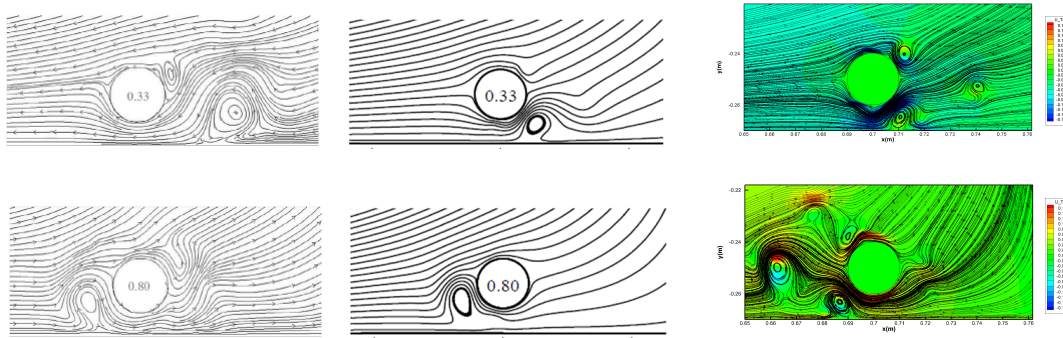


Figure 3: Fixed cylinder in Airy wave: Snapshots at  $t/T = 0.33$  and  $t/T = 0.8$ . Left: numerical streamlines from [8] with 50 cells per diameter - Middle: numerical streamlines from [21] - Right: numerical streamlines obtained with SWENSE-WCCH for 200 cells per diameter.

## Conclusion

In the first part of the present paper, the SWENSE method has been extended from an incompressible Navier-Stokes formulation to a weakly-compressible one. The original weakly-compressible Navier-Stokes equations are seen as a combination of an incident and a disturbed solution. As only low Mach numbers are considered, an hypothesis of weak variation of the density has been introduced. Only the disturbed solution needs to be computed, in addition to advection terms of the disturbed solution along the imposed incident velocity. The proposed weakly-compressible SWENSE formulation has then been carefully derived and validated in a Cartesian grid explicit solver. It will need to be further studied, namely in cases involving more complex incident waves and 3D cases. Future researches will be mainly oriented towards the implementation of the SWENSE method within a multiphase solver, and its application to ocean and naval engineering problems.

## References

- [1] M. Berger, M. J. Aftosmis, and S. Allmaras. Progress towards a Cartesian cut-cell method for viscous compressible flow. In *Proceedings of the AIAA Conference Paper2012-1301*, 2012.
- [2] P. Bigay, G. Oger, P-M Guilcher, and D. Le Touzé. A weakly-compressible Cartesian grid approach for hydrodynamic flows. 2017.
- [3] G. Ducrozet, F. Bonnefoy, D. Le Touzé, and P. Ferrant. Implementation and validation of nonlinear wave maker models in a HOS numerical wave tank. *International Journal of Offshore and Polar Engineering*, 16:pp. 161–167, 2006.
- [4] P. Ferrant. Fully non-linear interactions of longcrested wave packets with a three-dimensional body. In *Proceedings of the 22nd ONR Symposium on Naval Hydrodynamics*, pages 403–415, 1998.
- [5] P. Ferrant, L. Gentaz, B. Alessandrini, and D. Le Touzé. A potential/RANSE approach for regular water wave diffraction about 2d structures. *Ship Technology Research*, 50(4):165–171, 2003.
- [6] M. Gouin, G. Ducrozet, and P. Ferrant. Propagation of 3d nonlinear waves over an elliptical mound with a High-Order Spectral method. *European Journal of Mechanics-B/Fluids*, 63:9–24, 2017.
- [7] M. Gouin, G. Oger, and D. Le Touzé. Swense method in a weakly-compressible cartesian grid approach. *Journal of Computational Physics*, 2017 (submitted).
- [8] J. Inverno, M.G. Neves, E. Didier, and J. L. Lara. Numerical simulation of wave interacting with a submerged cylinder using a 2d RANS model. *Journal of Hydro-environment Research*, 12:1 – 15, 2016.
- [9] A. Jarno-Druaux, A. Sakout, and E. Lambert. Interference between a circular cylinder and a plane wall under waves. *Journal of Fluids and Structures*, 9(2):215 – 230, 1995.
- [10] B. van Leer. Towards the ultimate conservative difference scheme II. Monotonicity and conservation combined in a second-order scheme. *Journal of Computational Physics*, 14:361–370, 1974.
- [11] X.-D. Liu, S. Osher, and T. Chan. Weighted essentially non-oscillatory schemes. *Journal of Computational Physics*, 115:200–212, 1994.
- [12] R. Luquet, G. Ducrozet, L. Gentaz, P. Ferrant, and B. Alessandrini. Application of the SWENSE method to seakeeping simulations in irregular waves. In *9th Numerical Ship Hydrodynamics Conference Ann Arbor, Michigan, France, 2007*.
- [13] S. Marrone, A. Colagrossi, A. Di Mascio, and D. Le Touzé. Prediction of energy losses in water impacts using incompressible and weakly compressible models. *Journal of Fluids and Structures*, 54:802 – 822, 2015.
- [14] C. Monroy, G. Ducrozet, F. Bonnefoy, A. Babarit, L. Gentaz, and P. Ferrant. RANS simulations of CALM buoy in regular and irregular seas using SWENSE method. *ISOPÉ-11-21-4-264*, December 2011.
- [15] G. Oger, D. Le Touzé, G. Ducrozet, J. Candelier, and P.-M. Guilcher. A Coupled SPH-Spectral Method for the Simulation of Wave Train Impacts on a FPSO. (45400):V002T08A088, 2014.
- [16] G. Reliquet, A. Drouet, P.-E. Guillerm, E. Jacquin, L. Gentaz, and P. Ferrant. Simulation of wave-body interaction using a single phase Level Set function in the SWENSE method. In *Proceedings of the 32nd International conference on Ocean, Offshore and Arctic Engineering (OMAE), Nantes, France, 2013*.
- [17] M.M. Rienecker and J.D. Fenton. A Fourier approximation method for steady water waves. *Journal of Fluid Mechanics*, 104:119–137, 1981.
- [18] B.M. Sumer and J. Fredsøe. *Hydrodynamics around cylindrical structures*, volume 26. World scientific, 2006.
- [19] V. A. Titarev and E. F. Toro. Finite-Volume WENO schemes for three dimensional conservation laws. *Journal of Computational Physics*, 201:238–260, 2004.
- [20] V. Vukcevic, H. Jasak, and S. Malenica. Decomposition model for naval hydrodynamic applications, Part I: Computational method. *Ocean Engineering*, 121:37 – 46, 2016.
- [21] M. Zhao, L. Cheng, and H. Ah. A finite element solution of wave forces on a horizontal circular cylinder close to the sea-bed. *Journal of Hydrodynamics, Ser. B*, 18(3):139 – 145, 2006.